A&A 430, 655–668 (2005)
DOI: 10.1051/0004-6361:20041274

Astronomy & Astrophysics

First stars VI – Abundances of C, N, O, Li, and mixing in extremely metal-poor giants. Galactic evolution of the light elements⋆

M. Spite[1], R. Cayrel[1], B. Plez[2], V. Hill[1], F. Spite[1], E. Depagne[3], P. François[1], P. Bonifacio[4], B. Barbuy[5], T. Beers[6], J. Andersen[7,8], P. Molaro[4], B. Nordström[7,9], and F. Primas[10]

[1] GEPI, Observatoire de Paris-Meudon, 92125 Meudon Cedex, France
e-mail: monique.spite@obspm.fr
[2] GRAAL, Université de Montpellier II, 34095 Montpellier Cedex 05, France
[3] European Southern Observatory (ESO), 3107 Alonso de Cordova, Vitacura, Casilla 19001, Santiago 19, Chile
[4] Osservatorio Astronomico di Trieste, INAF, via G.B. Tiepolo 11, 34131 Trieste, Italy
[5] IAG, Universidade de Sao Paulo, Depto. de Astronomia, rua do Matao 1226, Sao Paulo 05508-900, Brazil
[6] Department of Physics & Astronomy and JINA: Joint Institute for Nuclear Astrophysics, Michigan State University, East Lansing, MI 48824, USA
[7] Astronomical Observatory, NBIfAFG, Juliane Maries Vej 30, 2100 Copenhagen, Denmark
[8] Nordic Optical Telescope Scientific Association, Apartado 474, 38 700 Santa Cruz de La Palma, Spain
[9] Lund Observatory, Box 43, 221 00 Lund, Sweden
[10] European Southern Observatory, Karl Schwarzschild-Str. 2, 85749 Garching b. München, Germany

Received 11 May 2004 / Accepted 21 September 2004

Abstract. We have investigated the poorly-understood origin of nitrogen in the early Galaxy by determining N abundances from the NH band at 336 nm in 35 extremely metal-poor halo giants, with carbon and oxygen abundances from Cayrel et al. (2004, A&A, 416, 1117), using high-quality ESO VLT/UVES spectra (30 of our 35 stars are in the range $-4.1 < [Fe/H] < -2.7$ and 22 stars have $[Fe/H] < -3.0$). N abundances derived both from the NH band and from the CN band at 389 nm for 10 stars correlate well, but show a systematic difference of 0.4 dex, which we attribute to uncertainties in the physical parameters of the NH band (line positions, gf values, dissociation energy, etc.). Because any dredge-up of CNO processed material to the surface may complicate the interpretation of CNO abundances in giants, we have also measured the surface abundance of lithium in our stars as a diagnostic of such mixing. Our sample shows a clear dichotomy between two groups of stars. The first group shows evidence of C to N conversion through CN cycling and strong Li dilution, a signature of mixing; these stars are generally more evolved and located on the upper Red Giant Branch (RGB) or Horizontal Branch (HB). The second group has [N/Fe] < 0.5, shows no evidence for C to N conversion, and Li is only moderately diluted; these stars belong to the lower RGB and we conclude that their C and N abundances are very close to those of the gas from which they formed in the early Galaxy, they are called "unmixed stars". The [O/Fe] and [(C+N)/Fe] ratios are the same in the two groups, confirming that the differences between them are caused by dredge-up of CN-processed material in the first group, with negligible contributions from the O-N cycle. The "unmixed" stars reflect the abundances in the early Galaxy: the [C/Fe] ratio is constant (about +0.2 dex) and the [C/Mg] ratio is close to solar at low metallicity, favouring a high C production by massive zero-metal supernovae. The [N/Fe] and [N/Mg] ratios scatter widely. Their mean values in each metallicity bin decrease with increasing metallicity, but this trend could be a statistical effect. The larger values of these ratios define a flat upper plateau ([N/Mg] = 0.0, [N/Fe] = +0.1), which could reflect higher values within a wide range of yields of zero-metal SNe II. Alternatively, by analogy with the DLAs, the lower abundances ([N/Mg] = −1.1, [N/Fe] = −0.7) could reflect generally low yields from the first SNe II, the other stars being N enhanced by winds of massive Asymptotic Giant Branch (AGB) stars. Since all the stars show clear [α/Fe] enhancements, they were formed before any significant enrichment of the Galactic gas by SNe Ia, and their composition should reflect the yields of the first SNe II. However, if massive AGB stars or AGB supernovae evolved more rapidly than SNe Ia and contaminated the ISM, our stars would also reflect the yields of these AGB stars. At present it cannot be decided whether primary N is produced primarily in SNe II or in massive AGB stars, or in both. The stellar N abundances and [N/O] ratios are compatible with those found in Damped Lyman-α (DLA) systems. They extend the well-known DLA "plateau" at [N/O] ≈ −0.8 to lower metallicities, albeit with more scatter; no star is found below the putative "low [N/α] plateau" at [N/O] ≈ −1.55 in DLAs.

Key words. Galaxy: abundances – Galaxy: halo – Galaxy: evolution – stars: abundances – stars: evolution – stars: supernovae: general

1. Introduction

Carbon, nitrogen, and oxygen – the CNO elements – are key players in the chemical evolution of galaxies. They are the most

⋆ Based on observations obtained with the ESO VLT under ESO programme ID 165.N-0276(A). This work has made use of the SIMBAD database.

abundant elements after hydrogen and helium and the most efficient coolants in the interstellar medium. Thus, understanding how the first CNO nuclei were synthesised is crucial for models of the first star formation and nucleosynthesis in the Universe after the Big Bang.

There is general consensus that oxygen is almost entirely contributed by massive type II SNe, primarily during the central hydrogen burning with some contribution from neon burning. Carbon can be produced in stars of all masses, essentially by He burning. In contrast to O and C, however, the initial formation of N is still not well understood (Pilyugin et al. 2003).

N is formed at the expense of C and O during hydrogen burning by the CNO cycle. If N is formed directly from He, it is called primary; if pre-existing C nuclei are required, it is called secondary. In massive stars, mixing (with or without stellar rotation) between the helium-burning layer (which produces C) and the hydrogen-burning layer can induce "primary" N formation; the yield may be very variable. In intermediate-mass stars with (approx. $4\ M_\odot < M < 8\ M_\odot$), abundant primary N may be produced during the AGB phase.

The production mechanisms of N are imprinted in the abundances of stars formed from the ejecta of massive progenitor stars. If the N production was secondary, the [N/O] ratio should increase with increasing metallicity. For primary N production, [N/O] should remain constant.

From a study of H II regions in irregular galaxies (Kobulnicky & Skillman 1996; Izotov & Thuan 1999), the [N/O] ratio does indeed appear to be constant at low metallicity, at least between [O/H] = −1.6 and −1.2, or about $-2.1 < [Fe/H] < -1.7$, suggesting that N is primary in this range. From the small dispersion of their [N/O] measurements, Izotov & Thuan argue in favor of N production by massive stars. However, this conclusion is challenged by observations of DLAs, which exhibit large scatter and, in particular, lower values of [N/O] than those of H II regions in irregular galaxies. Henry et al. (2000) could reproduce the plateau in [N/O] by assuming N production by AGB stars and different Star Formation Rates (SFRs), while Prochaska et al. (2002) proposed a scenario involving a different IMF at earlier epochs of star formation. The complex evidence suggests that primary production of N, if confirmed, might require production by both massive stars or AGBs.

Recently, however, Chiappini et al. (2003) questioned the very presence of the plateau and its significance as an evolutionary curve. They further stressed that while the [N/O] vs. [O/H] diagram for DLAs and H II regions is often interpreted as an evolutionary diagram with [O/H] as the time axis, it does in fact represent final abundances achieved by objects that evolved in completely different ways from each other. Hence, the best way to determine the lower limit of the [N/O] ratio is to measure it in very old Galactic stars.

Among early discussions of the Galactic evolution of N in halo stars, Tomkin & Lambert (1984) analysed 14 disk and halo dwarfs in the range $-2.3 \le [Fe/H] \le -0.3$, using the ultraviolet NH band. They found [N/Fe] = −0.25, [C/Fe] = −0.21, and an average [N/C] = −0.02 ± 0.3. Laird (1985) analysed 116 dwarfs with $-2.45 \le [Fe/H] \le +0.5$ from observations of the G band of CH and the violet NH band at low resolution and found [C/Fe] = −0.22 ± 0.14 and [N/Fe] = −0.67 ± 0.21. In both studies, the N abundances were corrected by +0.65 dex and C by +0.2 dex in order to obtain [N/Fe] = [C/Fe] = 0 at solar metallicity. Carbon et al. (1987) also observed the CH band and violet NH band at low resolution in 83 dwarfs, including 27 in the range $-2.7 \le [Fe/H] \le -2.0$. Assuming [O/Fe] = +0.6 (important for the derived C abundance), they found [C/Fe] = −0.03 ± 0.18, and [N/Fe] = −0.45 ± 0.28. These three sets of data suggested that Nitrogen showed a behaviour as a primary element at the low metallicities studied ($-2.7 \le [Fe/H] \le -2.0$).

Very recently, Israelian et al. (2004) measured nitrogen abundances in 31 unevolved stars with $-3.05 \le [Fe/H] \le -0.35$, using the near-UV NH band. As only four stars in their sample have $[Fe/H] < -2.5$, their metallicity range is complementary to the present work (see below). Israelian et al. find no trend of [N/Fe] vs. [Fe/H], suggesting also primary N production. For stars of higher metallicity ($[O/H] > -1.8$) they find a significant slope of [N/O] versus [O/H], indicative of secondary behaviour. Because they derive [N/O] from similar analyses of the near-UV bands of OH and NH, systematic errors in the molecular analysis should at least partly cancel.

On this background, the aim of the present paper is to determine C and N abundances in stars from the very earliest phases of the evolution of the Galaxy. Cayrel et al. (2004, hereafter Paper V) already analysed the abundances of 17 elements from C to Zn in 35 extremely metal-poor (XMP) stars ($-4.0 < [Fe/H] < -2.7$). For most elements, the diagrams of [X/Fe] (or [X/Mg]) vs. [Fe/H] (or [Mg/H]) showed very small dispersion, and the trends (or absence of trends) of the different element ratios with metallicity could be determined rather easily. In contrast, the relations [C/Fe] vs. [Fe/H] (or [C/Mg] vs. [Mg/H]) showed so large scatter that no conclusions on the production of C could be drawn. N abundances were measured from CN, but this band was only detected in six stars.

In this paper we use the high UV efficiency of the VLT spectrograph UVES to push the study of the Galactic evolution of N a step further. Using the NH band at 336 nm allows us to measure N abundances in the same large sample of extremely metal-poor halo giants as that of Cayrel et al. (2004): 35 stars with $-4.1 \le [Fe/H] \le -2.0$, 30 of which have $-4 < [Fe/H] < -2.7$ (and 22 have $[Fe/H] < -3.0$). At these metallicities it is essentially impossible to detect the NH band in main-sequence or turnoff stars (unless they have a strong N excess), so the less-evolved, unmixed giants in our sample offer essentially the only way to measure N at such low metallicities.

Mixing of the outer layers in these stars may invalidate conclusions drawn from an abundance analysis of their surfaces. Its importance can be estimated from several indicators, in particular from the abundance of lithium, which is rapidly destroyed if convection drives it to regions with temperatures above $\sim 2.5 \times 10^6$ K. For example ^{7}Li is destroyed in about 97% of the mass of a $0.9\ M_\odot$ very metal-poor star during its main-sequence evolution. When the outer convective zone deepens, the remaining 3% is diluted by the full mass of the convective zone, and the surface Li abundance becomes a diagnostic of the depth of this convective zone. Accordingly, we have also measured Li abundances in our giants to distinguish between mixed and unmixed stars.

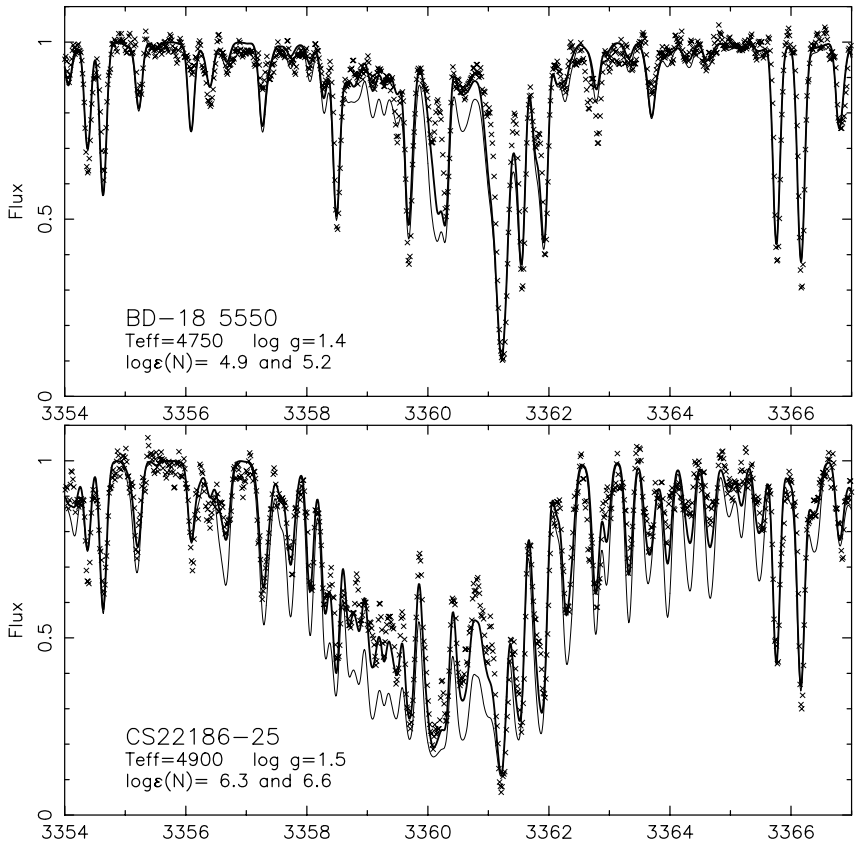

Fig. 1. Reduced UVES spectra in the region of the NH band at 336 nm. Crosses represent the observed spectra, while the full lines show synthetic spectra computed for the best-fit N abundance as well as twice that value (thick and thin lines, respectively). The two stars have about the same metallicity, [Fe/H] = −3.06 (BD-18:5550) and [Fe/H] = −3.00 (CS 22186–025).

In Sect. 2 we describe the observations, and Sect. 3 presents the analysis of the data. Section 4 discusses mixing in these stars, while Sect. 5 considers the abundances of the CNO elements in the early Galaxy and presents a comparison of our results with data from DLAs. Section 6 is a brief summary of our results and conclusions.

2. Observations and reductions

The observations were performed during several observing runs from April 2000 to November 2001 with the VLT-UT2 and UVES (Dekker et al. 2000), at a resolving power of $R = 47\,000$ at 400 nm. The spectra were reduced using the UVES context (Ballester et al. 2000) within MIDAS. Details of the observing and reduction procedures are presented in Paper V (Cayrel et al. 2004). Taking advantage of the high UV efficiency of UVES allows us to measure the NH band at 336 nm in most of our stars.

The signal-to-noise ratio of the spectra is difficult to estimate in this very crowded region, but is typically $S/N \approx 30$ (per pixel). An example of the spectrum in the region of the NH band is shown in Fig. 1.

3. Abundance analysis

As described in Paper V, we carried out a classical LTE analysis using OSMARCS model atmospheres (Gustafsson et al. 1975; Plez et al. 1992; Edvardsson et al. 1993; Asplund et al. 1997; Gustafsson et al. 2003). Since our analysis uses 1D models we adopted, as in Paper V, the solar abundances as obtained also from 1D models, i.e., $\log \epsilon$ (O) = 8.74, $\log \epsilon$ (C) = 8.52, $\log \epsilon$ (N) = 7.92, and the values for other elements from Grevesse & Sauval (1998).

Abundances were derived using the current version of the Turbospectrum code (Alvarez & Plez 1998), which accounts properly for continuum scattering (see Paper V), a feature that is particularly important in the violet part of the spectrum. For the CH, CN, and NH bands the abundances of C and N were determined from spectrum synthesis. Abundances of O from the forbidden line at 630.031 nm and of Li from the resonance line have been derived directly from the equivalent widths of these lines.

3.1. Atmospheric parameters

The procedures used to derive $T_{\rm eff}$, $\log g$, and the microturbulent velocity v_t have been explained in detail in Paper V, Sect. 3. Briefly, $T_{\rm eff}$ was derived from broadband photometry ($B - V$, $V - R$, $V - I$, $V - K$, $J - K$), calibrated by the IRFM method (Alonso et al. 1999). The $\log g$ value was obtained by requiring that identical Fe and Ti abundances be derived from Fe I and Fe II, or Ti I, Ti II lines, respectively, and v_t was determined to eliminate any abundance trend of the Fe I lines with equivalent width.

Table 1. Adopted model parameters ($T_{\rm eff}$, log g, v_t, [Fe/H]) and light element abundances for the programme stars. For Li, C and N the 1σ measurement error is given. The N abundances from the NH band in Col. 10 are raw values, to be corrected by −0.4 dex (see Sect. 3.2.3 and Fig. 4), the adopted values of [N/H] are given in Col. 11. Remark "m" in the last column identifies stars considered to be mixed (see Sect. 4.1). The errors indicated in this table are only the measurement errors.

	Star	$T_{\rm eff}$	log g	v_t	[Fe/H]	log$N$(Li)	[C/H]	[N/H] (CN)	[N/H] (NH)	adopt. [N/H]	[O/H]	$[\frac{\rm C+N}{\rm Fe}]$	R
1	HD 2796	4950	1.5	2.1	−2.47	<−0.30	−2.97 ± 0.06	−1.52	−1.22 ± 0.08	−1.62	−1.97	0.14	m
2	HD 122563	4600	1.1	2.0	−2.82	<−0.60	−3.29 ± 0.05	−2.12	−1.72 ± 0.15	−2.12	−2.20	0.04	m
3	HD 186478	4700	1.3	2.0	−2.59	<−0.50	−2.89 ± 0.07	−2.02	−1.57 ± 0.12	−1.97	−1.84	0.01	m
4	BD +17:3248	5250	1.4	1.5	−2.07	<0.00	−2.44 ± 0.05	−1.37	−1.02 ± 0.10	−1.42	−1.38	0.00	m
5	BD −18:5550	4750	1.4	1.8	−3.06	0.75 ± 0.04	−3.08 ± 0.04	–	−3.02 ± 0.10	−3.42	−2.64	−0.08	
6	CD −38:245	4800	1.5	2.2	−4.19	<−0.40	<−4.52	–	−2.72 ± 0.20	−3.12	–	<0.35	m
7	BS 16467–062	5200	2.5	1.6	−3.77	0.80 ± 0.08	−3.52 ± 0.12	–	< −2.92	<−3.32	–	–	
8	BS 16477–003	4900	1.7	1.8	−3.36	0.90 ± 0.04	−3.07 ± 0.08	–	< −3.22	<−3.62	–	–	
9	BS 17569–049	4700	1.2	1.9	−2.88	<−0.30	−3.00 ± 0.05	−2.12	−1.62 ± 0.12	−2.02	–	0.22	m
10	CS 22169–035	4700	1.2	2.2	−3.04	<−0.35	−3.26 ± 0.05	−2.02	−1.62 ± 0.13	−2.02	–	0.32	m
11	CS 22172–002	4800	1.3	2.2	−3.86	0.32 ± 0.11	−3.86 ± 0.10	–	−3.22 ± 0.20	−3.62	−2.82	0.01	
12	CS 22186–025	4900	1.5	2.0	−3.00	<−0.15	−3.54 ± 0.10	–	−1.62 ± 0.08	−2.02	−2.41	0.23	m
13	CS 22189–009	4900	1.7	1.9	−3.49	0.54 ± 0.05	−3.18 ± 0.08	–	−2.82 ± 0.12	−3.22	–	0.25	
14	CS 22873–055	4550	0.7	2.2	−2.99	<−0.35	−3.72 ± 0.06	–	−1.52 ± 0.20	−1.92	−2.47	0.19	m
15	CS 22873–166	4550	0.9	2.1	−2.97	<−0.55	−3.10 ± 0.08	−1.92	−1.52 ± 0.20	−1.92	–	0.37	m
16	CS 22878–101	4800	1.3	2.0	−3.25	<−0.30	−3.54 ± 0.10	–	−1.52 ± 0.10	−1.92	–	0.58	m
17	CS 22885–096	5050	2.6	1.8	−3.78	0.83 ± 0.05	−3.52 ± 0.06	–	−3.12 ± 0.13	−3.52	–	0.20	
18	CS 22891–209	4700	1.0	2.1	−3.29	<−0.50	−3.94 ± 0.05	–	−1.77 ± 0.10	−2.17	−2.52	0.36	m
19	CS 22892–052	4850	1.6	1.9	−3.03	0.20 ± 0.09	−2.14 ± 0.06	−2.32	−2.12 ± 0.13	−2.52	−2.56	0.83	
20	CS 22896–154	5250	2.7	1.2	−2.69	1.15 ± 0.04	−2.46 ± 0.05	–	−2.52 ± 0.12	−2.92	−1.75	0.19	
21	CS 22897–008	4900	1.7	2.0	−3.41	0.90 ± 0.04	−2.85 ± 0.05	–	−2.77 ± 0.15	−3.17	–	0.45	
22	CS 22948–066	5100	1.8	2.0	−3.14	<0.00	−3.14 ± 0.10	–	−1.52 ± 0.10	−1.92	−2.25	0.61	m
23	CS 22949–037	4900	1.5	1.8	−3.97	<−0.30	−2.82 ± 0.10	−1.40	−1.32 ± 0.30	−1.82	−1.99	1.67	m
24	CS 22952–015	4800	1.3	2.1	−3.43	<−0.40	−4.02 ± 0.08	–	−1.72 ± 0.10	−2.12	–	0.54	m
25	CS 22953–003	5100	2.3	1.7	−2.84	0.80 ± 0.04	−2.54 ± 0.03	–	−2.32 ± 0.10	−2.72	−2.09	0.57	
26	CS 22956–050	4900	1.7	1.8	−3.33	0.97 ± 0.03	−3.06 ± 0.05	–	−2.62 ± 0.10	−3.02	−2.21	0.26	
27	CS 22966–057	5300	2.2	1.4	−2.62	1.35 ± 0.03	−2.56 ± 0.05	–	−2.12 ± 0.12	−2.52	−1.63	0.04	
28	CS 22968–014	4850	1.7	1.9	−3.56	0.52 ± 0.08	−3.31 ± 0.06	–	−2.92 ± 0.10	−3.32	−2.66	0.25	
29	CS 29491–053	4700	1.3	2.0	−3.04	<−0.10	−3.31 ± 0.05	−2.32	−1.82 ± 0.15	−2.22	−2.28	0.16	m
30	CS 29495–041	4800	1.5	1.8	−2.82	0.38 ± 0.09	−2.89 ± 0.06	–	−2.02 ± 0.10	−2.42	−2.14	0.05	
31	CS 29502–042	5100	2.5	1.5	−3.19	0.90 ± 0.05	−3.03 ± 0.04	–	−3.22 ± 0.20	−3.62	–	0.15	
32	CS 29516–024	4650	1.2	1.7	−3.06	0.33 ± 0.04	−3.12 ± 0.05	–	−3.42 ± 0.20	−3.82	−2.44	−0.09	
33	CS 29518–051	5200	2.6	1.4	−2.69	<−0.10	−2.82 ± 0.05	–	−1.47 ± 0.15	−1.87	−1.89	0.24	m
34	CS 30325–094	4950	2.0	1.5	−3.30	<−0.25	−3.30 ± 0.05	–	−2.72 ± 0.18	−3.12	−2.58	0.00	
35	CS 31082–001	4825	1.5	1.8	−2.91	0.85 ± 0.05	−2.69 ± 0.05	<−2.70	−3.02 ± 0.10	−3.42	−2.31	0.13	

3.2. Abundances of the light elements

3.2.1. Lithium

The Li line at 670.7 nm is visible in about half of our stars. Table 1 lists the derived Li abundances for these stars, and upper limits for the remaining stars.

Figure 2 shows the Li feature in the neutron-capture-rich XMP star CS 22892–052 (Sneden et al. 2003). We measure an equivalent width of 3.3 mÅ, in excellent agreement with the value $W_{\rm Li}$ = 3.5 mÅ by Sneden et al. (2003).

3.2.2. Carbon and oxygen

Carbon and oxygen abundances for our stars were carefully determined in Paper V (specifically in Sects. 4.1 and 4.2) and are reproduced in Table 1 (see also Barbuy et al. 2003).

The O abundance was derived from the [O I] line at 630.031 nm (Table 1), generally considered to be the most reliable O abundance indicator since it is insensitive to non-LTE effects. However, these values were computed with classical 1D models, and the line has been shown to be sensitive to hydrodynamical (3D) effects: the [O/Fe] ratio based on the

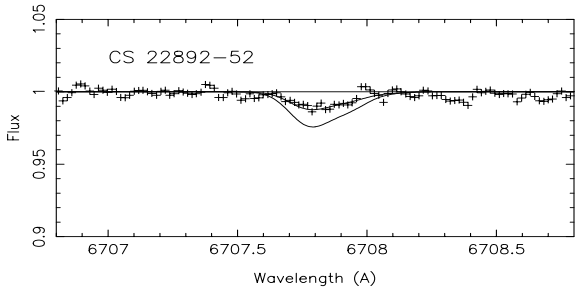

Fig. 2. Observed spectrum of CS 22892-52 near the Li line at 670.7 nm (crosses), and synthetic spectra computed with log N(Li) = 0.15 and 0.45 (thick and thin lines, respectively).

[O I] line is expected to decrease when computed with 3D models. So far, explicit 3D corrections have only been computed for dwarfs (Nissen et al. 2002). Following these authors, at least the sign of the correction should not change in giants; and we assume, as a first approximation, that the correction is the same as for dwarfs. The 1D values of [O/Fe] = [O/H]–[Fe/H] (Table 1) should then be corrected by about −0.23 dex (see Paper V).

C abundances were determined by a synthetic spectrum fit to the G band of CH (see Paper V).

Figure 3 shows the [C/Fe] and [C/Mg] ratios as functions of [Fe/H] and [Mg/H]. They show substantially larger scatter around the mean value than all other elements studied in Paper V. Even if the two peculiar stars with very strong C enhancements are excluded, i.e. CS 22892–052 (Sneden et al. 1996, 2000, 2003) and CS 22949–037 (McWilliam et al. 1995; Norris et al. 2001; Depagne et al. 2002), the scatter remains very large ($\langle$[C/Fe]$\rangle$ = −0.09 and σ = 0.373). In Paper V we studied a subset of stars with $T_{\rm eff}$ > 4800 K (the hotter, less evolved part of the RGB), but the scatter remained almost constant, with $\langle$[C/Fe]$\rangle$ = +0.01 and σ = 0.367 (see Figs. 5 and 12 in Paper V).

We conclude that either the gas from which the XMP stars formed had a wide range of C abundances, or the initial composition in the atmosphere of the stars has been altered by subsequent mixing episodes. In the latter case we would also expect a correspondingly large scatter in the relation of [N/Fe] vs. [Fe/H].

3.2.3. Nitrogen

In Paper V, N abundances were computed from the BX band of CN at 388.8 nm. This band is extremely weak in most of our sample and the nitrogen abundance had been computed in only six stars. After a careful examination of the spectra, we could in fact detect the CN band and measure it, in ten stars (Table 1).

Moreover in the present paper, we use the lines of the violet $A^3\Pi_i - X^3\Sigma^-$ NH band at 336 nm (see Fig. 1), which is not only more readily measurable but also insensitive to the C and O abundances (see e.g. Sneden 1973 or Norris et al. 2002). We have adopted the Kurucz (2001) data for the NH molecule (Table 1, Fig. 4), in particular a dissociation energy of 3.47 eV (Huber & Herzberg 1979).

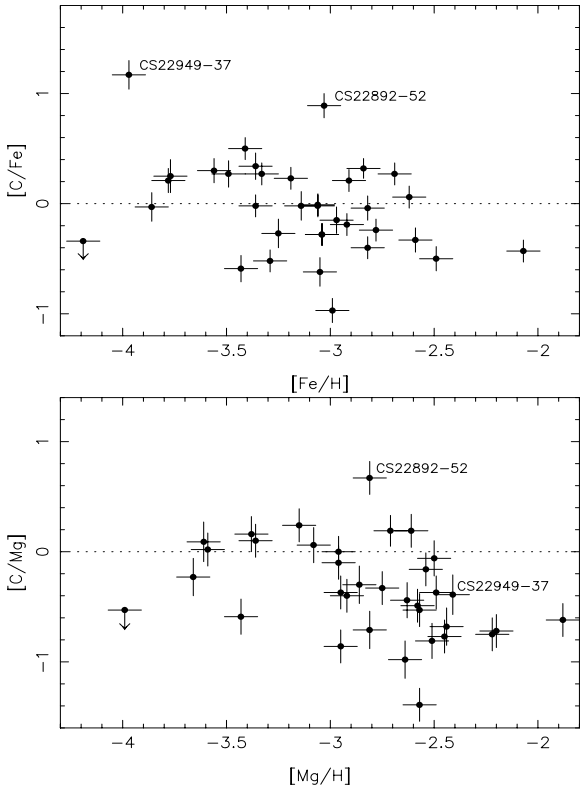

Fig. 3. [C/Fe] and [C/Mg] vs. [Fe/H] and [Mg/H]. Both diagrams show far more scatter than seen for other elements in Paper V. The peculiar "carbon-rich" stars CS 22949–037 and CS 22892-052 are labelled; they cannot be directly compared to the other stars of the sample.

Figure 4 compares the N abundances derived from the NH and CN molecular bands. The correlation is good, but there is a systematic difference of about 0.4 dex, well above the internal errors. The reason for this discrepancy is unclear, but we recall that the physical parameters (line positions, gf values, etc.) of the NH band are not yet well established. We use a dissociation energy of 3.47 eV (Huber & Herzberg 1979), while Sneden (1973) and Norris et al. (2002) preferred a value of 3.21 eV. However, adopting a lower dissociation energy would further *increase* our N abundances from NH and the discrepancy with the results from CN. In contrast, the dissociation energy and other parameters of the CN molecule seem to be better established. We have adopted $D_{\rm CN}$ = 7.76 eV (Huber & Herzberg 1979), which is supported by more recent experimental (e.g. 7.74 ± 0.02, Huang et al. 1992) and theoretical values (e.g. 7.72 ± 0.02, Pradhan et al. 1994).

We conclude that our nitrogen abundances from the NH band (Table 1) should be corrected by −0.4 dex and use these corrected values in the following discussions.

Figure 5 shows the relations [N/Fe] vs. [Fe/H] and [N/Mg] vs. [Mg/H]. Here again the scatter is extremely large, even greater than in the case of C.

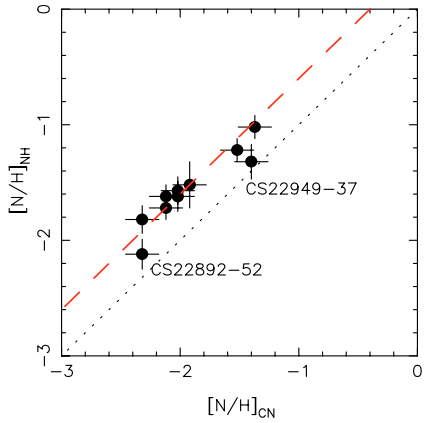

Fig. 4. [N/H] values derived from the CN and NH bands. The correlation is good, but shows a systematic shift of about 0.4 dex. The two carbon-rich stars are identified.

3.3. Errors due to the uncertainty of the atmospheric parameters

Except for measurement errors, the main source of error in the C, N, and Li abundances is the uncertainty in $T_{\rm eff}$, which is about 80 K (Paper V). For given $T_{\rm eff}$, the ionization equilibrium constrains log g with an internal error of 0.1 dex, while v_t is constrained to within ± 0.2 km s^{-1}. In Table 2 we list the uncertainties in log N(Li), [C/Fe], [N/Fe] and also [(C+N)/Fe] and [C/N] arising from these sources for two stars, HD 122563 ($T_{\rm eff}$ = 4600 K) and CS 22948–066 ($T_{\rm eff}$ = 5100 K), at the cool and warm end of our sample.

The errors are very similar in both cases and thus are practically independent of the temperature of the star between 4600 and 5100 K. Since log g is derived from the ionization equilibrium, it is not independent of $T_{\rm eff}$, so a change in $T_{\rm eff}$ also affects log g. The total error budget therefore contains significant covariance terms. To minimise these effects we have computed [C/Fe], [N/Fe] and [(C+N)/Fe] relative to Fe I for each model, since these abundances are affected similarly by a change in temperature.

The total error has been approximated by $\sqrt{(}\sigma_{\rm m}^2+\sigma_{\rm T}^2+\sigma_{\rm g}^2+\sigma_{\rm v}^2)$ where $\sigma_{\rm m}$ is the measurement error (Table 1) and $\sigma_{\rm T}$, $\sigma_{\rm g}$, $\sigma_{\rm v}$ are derived from Table 2 (Δ(D − A), Δ(B − A), Δ(C − A)). Note that in Table 2 the assumed change in $T_{\rm eff}$ is 100 K.

4. Mixing in metal-poor giants

4.1. Evidence from carbon and nitrogen

The aim of this paper is to study the synthesis of the light elements in the Galaxy at the earliest times, i.e. their abundances in gas that was enriched by the first type II supernovae. Generally, the convective atmosphere of a cool star is a good tracer of the chemical composition of the interstellar gas at the time and place of its formation. However, in giant stars material from deeper layers may be dredged to the surface and thereby alter the initial composition (e.g. Gratton et al. 2000), so we must carefully check if such mixing has occurred in our stars.

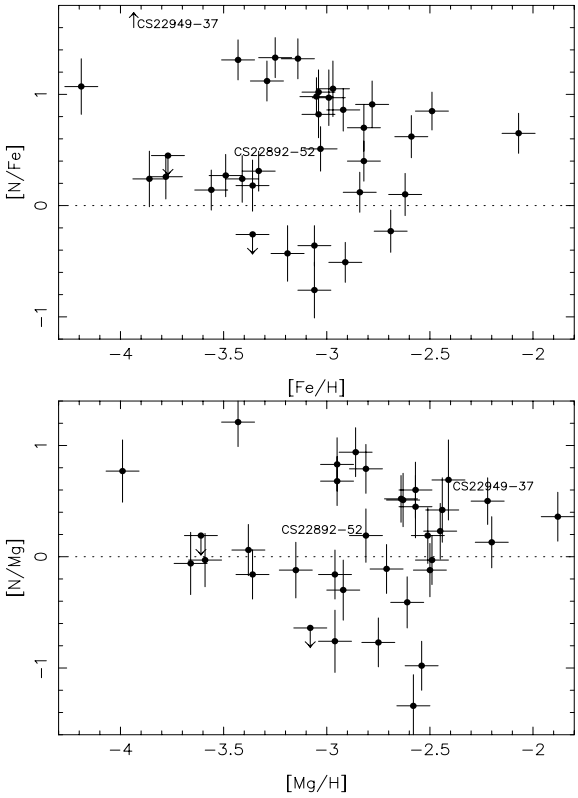

Fig. 5. [N/Fe] vs. [Fe/H] and [N/Mg] vs. [Mg/H] for our sample. The scatter of the points is even larger than in Fig. 3 (the scale of both figures is the same).

In dredged-up matter that has been processed by the CNO cycle, N has been produced at the expense of C, and the atmosphere of the star becomes "N rich" and "C poor" relative to its initial composition (thus, mixing during any first dredge-up episodes cannot explain the C-rich stars, especially in our low-mass stars.)

Figure 6 shows [N/Fe] vs. [C/Fe] for all stars in our sample. The stars clearly fall in two separate groups: the apparently unmixed stars with [C/Fe] $\geq$ 0.0 and [N/Fe] $<$ +0.5, and stars with [C/Fe] $<$ 0.0 and [N/Fe] $>$ +0.5 which show evidence of mixing. These ratios are, by themselves, no proof that the stars of the second group have been mixed internally; the gas from which they were formed *could* have had this composition. However, for simplicity we will continue to refer to these two groups as the unmixed and mixed stars, respectively. The "mixed" stars are identified by an "m" in Table 1 (last column).

4.2. Evidence from the C/N ratio

Because the CNO process turns C into N, the [C/N] ratio is a sensitive indicator of mixing. Figure 7 shows the [C/N] ratio vs. $T_{\rm eff}$. Like in Fig. 6, the mixed and unmixed stars are well separated. Note that most of the unmixed stars have $T_{\rm eff} \geq 4800$ K (cf. Paper V, Sect. 4.1).

Two stars in our sample are known to be C rich: CS 22892–052 (Sneden et al. 2003) falls close to the unmixed stars in Fig. 6, while CS 22949–037 (Depagne et al. 2002) is

Table 2. Changes (Δ) in the derived N abundance caused by errors in model atmosphere parameters for HD 122563, a cool star, and CS 22948-066 (hotter). A is the adopted model; B, C, and D vary log g, v_t, and $T_{\rm eff}$ individually as shown, while in model E, log g and v_t have been re-adjusted for consistency with the lower $T_{\rm eff}$ (see also Paper V, Tables 6 and 7).

HD 122563				
A: $T_{\rm eff}$ = 4600 K, log g = 1.0 dex, vt = 2.0 km s^{-1}				
B: $T_{\rm eff}$ = 4600 K, log g = 0.9 dex, vt = 2.0 km s^{-1}				
C: $T_{\rm eff}$ = 4600 K, log g = 1.0 dex, vt = 1.8 km s^{-1}				
D: $T_{\rm eff}$ = 4500 K, log g = 1.0 dex, vt = 2.0 km s^{-1}				
E: $T_{\rm eff}$ = 4500 K, log g = 0.6 dex, vt = 1.8 km s^{-1}				
	Δ_{B-A}	Δ_{C-A}	Δ_{D-A}	Δ_{E-A}
[Fe/H]	0.03	0.03	–0.11	0.03
log$N$(Li)	0.01	0.00	–0.12	–0.06
log$N$(C)	0.04	0.00	–0.23	–0.08
[C/Fe I]	0.02	–0.09	–0.03	–0.05
log$N$(N)	0.05	0.00	–0.30	–0.05
[N/Fe I]	0.05	–0.13	–0.14	–0.06
[C/N]	–0.01	0.00	0.10	0.00
[(C + N)/Fe I]	0.07	–0.02	–0.24	0.05
CS 22948–066				
A: $T_{\rm eff}$ = 5100 K, log g = 1.8 dex, vt = 2.0 km s^{-1}				
B: $T_{\rm eff}$ = 5100 K, log g = 1.7 dex, vt = 2.0 km s^{-1}				
C: $T_{\rm eff}$ = 5100 K, log g = 1.8 dex, vt = 1.8 km s^{-1}				
D: $T_{\rm eff}$ = 5000 K, log g = 1.8 dex, vt = 2.0 km s^{-1}				
E: $T_{\rm eff}$ = 5000 K, log g = 1.5 dex, vt = 2.0 km s^{-1}				
	Δ_{B-A}	Δ_{C-A}	Δ_{D-A}	Δ_{E-A}
[Fe/H]	–0.02	+0.02	–0.05	–0.11
log$N$(Li)	0.01	0.00	–0.11	–0.10
log$N$(C)	+0.04	0.00	–0.20	–0.10
[C/Fe I]	+0.04	–0.05	–0.09	+0.00
log$N$(N)	+0.05	0.00	–0.30	–0.10
[N/Fe I]	+0.05	–0.05	–0.19	–0.01
[C/N]	–0.01	0.00	0.07	–0.03
[(C + N)/Fe I]	0.07	–0.02	–0.24	0.01

quite peculiar, as its huge N abundance is suggestive of mixing (consistent with its low ^{12}C/^{13}C ratio), yet it falls quite far from the other mixed stars. None of these two stars appears unusual in Fig. 7, however.

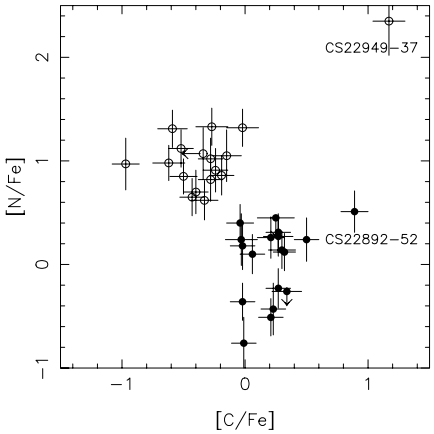

Fig. 6. [N/Fe] vs. [C/Fe] for our sample. Two groups are clearly separated: the "mixed" stars ([N/Fe] > 0.5) shown as open circles, and the "unmixed" stars ([N/Fe] < 0.5) shown as dots (both with error bars). CS 22892-52 and CS 22949-37 are the two peculiar carbon-rich stars.

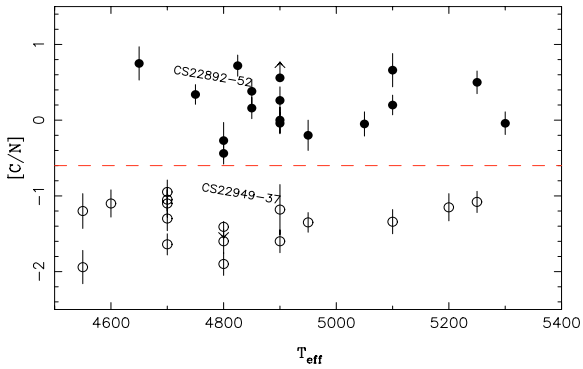

Fig. 7. [C/N] vs. $T_{\rm eff}$ for the sample; symbols as in Fig. 6. The line [C/N] = −0.4 separates the mixed and unmixed stars. Stars with only upper limits on C and/or N abundance have been omitted. Note that most unmixed stars have $T_{\rm eff} \geq 4800$ K (cf. also Paper V, Sect. 4.1).

For three stars we have only upper abundance limits: CD–38:245 (C only), BS 16477-003 (N only), and BS 16467–032 (both C and N); they are marked with arrows in Fig. 6, but omitted in Fig. 7 as the [C/N] ratio is undefined in these stars.

4.3. Evidence from lithium

When low-mass stars, such as those in our sample, evolve through the subgiant and red giant branches, the surface convection zone progressively deepens. This mixes the stellar atmosphere with material from deeper layers in which Li has been depleted by nuclear burning, and reduces the observed Li abundance of the star. The degree of dilution increases as the convective zone penetrates deeper; thus, one expects a steady decline of the observed Li abundance as a star ascends the RGB (Pilachowski et al. 1993). If mixing of the surface material is deep enough to reach the layers where C is burned into N, the atmospheric Li will a fortiori burn away rapidly. The mixed stars should thus show much lower Li abundances than the unmixed stars. We have performed this test.

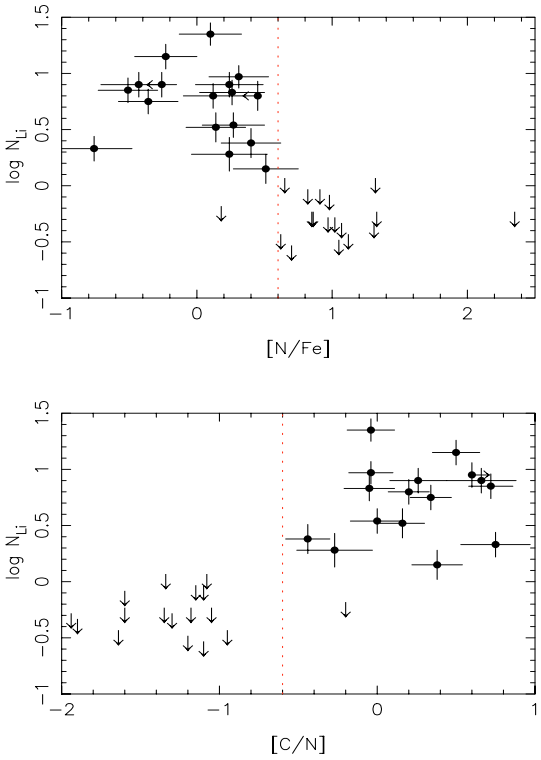

Fig. 8. Lithium abundances vs. [N/Fe] and [C/N] (symbols as in Fig. 6). All the mixed stars ([N/Fe] > 0.6 or [C/N] < −0.6; dotted lines) have destroyed their original Li.

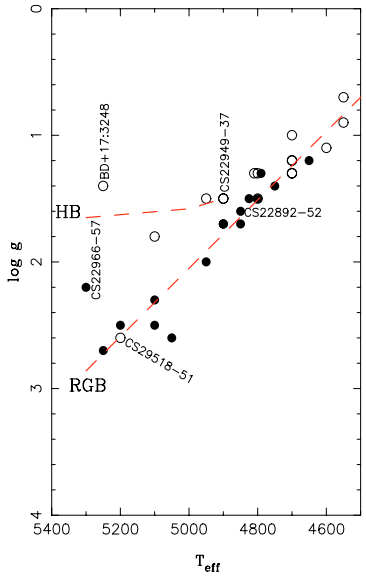

Fig. 9. log g vs. log $T_{\rm eff}$ diagram for the sample (symbols as in Fig. 6). The RGB and HB are fairly well-defined (dashed lines). At fixed $T_{\rm eff}$, the unmixed stars on the "low" RGB have higher log g than the mixed stars.

Figure 8 shows the observed surface abundance of Li as a function of [N/Fe] and [C/N]. The Li line is not detected in any of the mixed stars ([N/Fe] > 0.6 or [C/N] < −0.6), with an upper limit to the Li abundance of log N(Li) < 0. In contrast, we find log N(Li) > 0.15 for all the unmixed stars, with the sole exception of CS 30325–094 (log N(Li) < −0.25). Several effects may deplete the fragile Li in individual stars (rotation, gravity waves, binary interaction, ...) so we have not sought to clarify this single anomaly.

The consistent results from the [N/Fe] and [C/N] ratios and the Li abundance are strong evidence that the stars with [N/Fe] > 0.6 or [C/N] < −0.6 did experience mixing between deeper CNO-processed layers and the surface of the stars.

4.4. Location in the H-R diagram

Changes of abundances have been detected as stars evolve along the RGB in both globular cluster giants (Kraft 1994) and field stars (Gratton et al. 2000). It would thus be interesting to study the positions of our XMP stars in an H-R diagram to see at which phase of the evolution mixing has occurred. Unfortunately, these stars are too distant to have usable parallaxes, so their precise distances and luminosities are unknown.

However, the spectroscopic value of log g is a first-order indicator of the luminosity of the star. These values of log g may suffer from NLTE effects and thus be different from the true gravity, but Gratton et al. (2000) argue that NLTE corrections to log g are smaller than suggested in most previous literature; moreover, our stars lie in relatively narrow intervals of temperature and gravity, and NLTE effects on iron should be constant in the metallicity range of our stars (Korn et al. 2003). Therefore, any corrections would be similar for all the stars, and abundance trends with log g should be robust against NLTE effects.

Figure 9 shows the log g–log $T_{\rm eff}$ diagram for our sample. The unmixed stars form a fairly well-defined lower RGB, while virtually all stars on and above the HB have the spectroscopic characteristics of mixed stars, as previously found for moderately metal-poor field stars by Gratton et al. (2000). Three stars deviate from the general trend and are discussed in the following:

BD 17:3248, a mixed star strongly enriched in r-process elements (Cowan et al. 2002), has been classified as an RHB star (Bond 1999; Pilachowski et al. 1996; Alonso et al. 1998), in good agreement with its position in Fig. 9. In contrast, the Hipparcos parallax, π = 3.67 ± 1.5 mas, would place BD 17:3248 on the subgiant branch. However, Cowan et al. (2002) conclude, from Strömgren photometry, that the star is indeed highly evolved and the small Hipparcos parallax probably unreliable.

CS 22966-057, the hottest star of our sample, falls between the lower RGB and the HB. Our two spectra of this star from September and October 2001 yield radial velocities of +100.7 km s^{-1} and +103.0 km s^{-1}, a variation too large to be explained by our observational error, 0.5 km s^{-1}. This star is probably a binary.

CS 29518–051 falls on the low RGB, but has all the characteristics of a mixed star. A large error in its gravity is unlikely. Our single spectrum gives no information on any velocity variations, but the star clearly deserves close attention in the future.

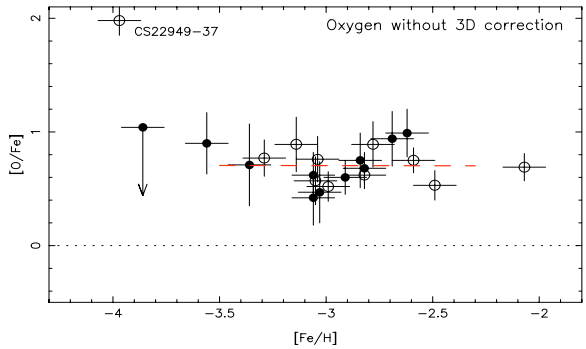

Fig. 10. [O/Fe] vs. [Fe/H] for the sample; symbols as in Fig. 6. The lack of any significant difference between mixed and unmixed stars is strong evidence that deep mixing has not occurred (the O abundances shown here are not corrected for 3D effects; cf. Paper V).

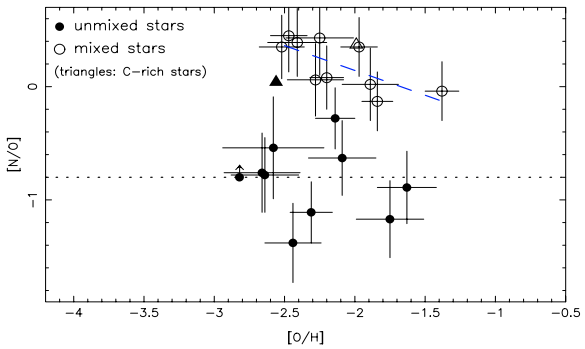

Fig. 11. [N/O] vs. [O/H] for the sample; symbols as in Fig. 6 (the carbon stars CS 22892–052 and CS22949–037 are shown as triangles). The [N/O] vs. [O/H] relation in the mixed stars is quite tight, [N/O] decreasing slightly with increasing [O/H] (dashed line). This suggests that the amount of N mixed to the surface does not depend strongly on metallicity.

4.5. Deep mixing and the early Galactic O abundance

A very deep mixing event might bring matter to the surface in which the O-N cycle has partially transformed O into N. It is thus interesting to compare the O abundances of the mixed and unmixed stars. As seen in Fig. 10, there is no significant difference in [O/Fe] between mixed and unmixed stars, and thus no evidence for contamination by deep mixing, as might occur in an AGB star of an earlier generation or in a hypothetical binary companion. This result is strong evidence that the O abundances determined in Paper V are indeed reliable indicators of the very early nucleosynthesis in the Galaxy.

4.6. CNO abundance ratios as detailed diagnostics of mixing

Figure 11 compares the [N/O] ratios in mixed and unmixed stars. As expected, [N/O] is systematically higher in the mixed stars, which have themselves produced N from C in the CN cycle. This additional N must therefore be of secondary origin[1]. Moreover, [N/O] and [O/H] are tightly correlated in all the mixed stars, in contrast with the large scatter observed in the unmixed stars. The large amount of N brought to the surface of the mixed stars has thus erased the large scatter of the initial N abundances. If this amount of N brought to the surface is assumed to be roughly independent of the metallicity of the star, the [N/O] ratio should decrease with increasing [O/H], as indeed seen in the data (Fig. 11, mixed stars, dashed line).

Because we find no evidence for processing by the O-N cycle in the mixed stars, if the excess of N is due to internal mixing it results only from the transformation of C nuclei into N. Thus we would expect that the mean value of the C+N abundance in the mixed and unmixed stars should be the same. Figure 12 shows that within errors this hypothesis is compatible with the observations. Note that the three mixed stars which stand out towards the high [(C+N)/Fe] ratios may belong to the horizontal branch.

[1] Note that a high N abundance in a metal-poor star does not necessarily imply that its atmosphere has been mixed with its CN processing interior. A few unmixed, N-rich, metal-poor stars are known to exist (e.g. G64-12, Israelian et al. 2004).

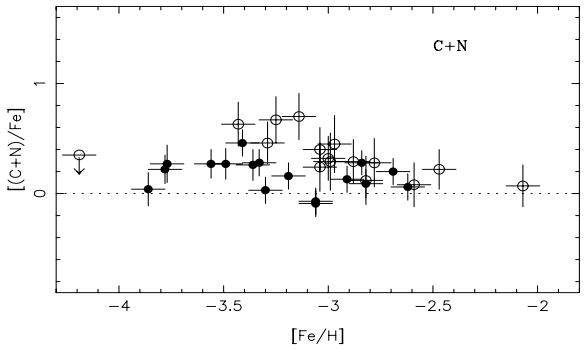

Fig. 12. [(C+N)/Fe] vs. [Fe/H]; symbols as in Fig. 6. The C+N abundance shows much smaller scatter than C or N alone (cf. Figs. 3 and 5). $\langle$[(C+N)/Fe]$\rangle \approx 0.25$ dex at low [Fe/H]. CS 22949–037 and CS 22892–052 are not shown here.

The peculiar C-rich stars CS 22949–037 and CS 22892–052 cannot be compared directly to the other stars of the sample. Both are included in Fig. 11, where CS 22892–052 has a rather high [N/O] ratio for an unmixed star while CS 22949-037 falls among the other mixed stars. Both have been omitted from Fig. 12, where they would fall far from the other stars in their groups.

The consistent evidence discussed above shows that our sample divides cleanly into two groups. In one, the stars have experienced mixing of their atmospheres over their lifetimes; in the other they have not.

5. CNO elements in the early Galaxy

We have presented strong evidence that the atmospheric CNO abundances of the unmixed stars represent the original abundances of these species in the gas from which the stars formed. We discuss the consequences of this identification in the following.

5.1. Carbon and the [C/O] ratio

Figure 13 shows the C abundance in our unmixed stars, with both Fe and Mg as reference elements. The [C/Fe] vs.

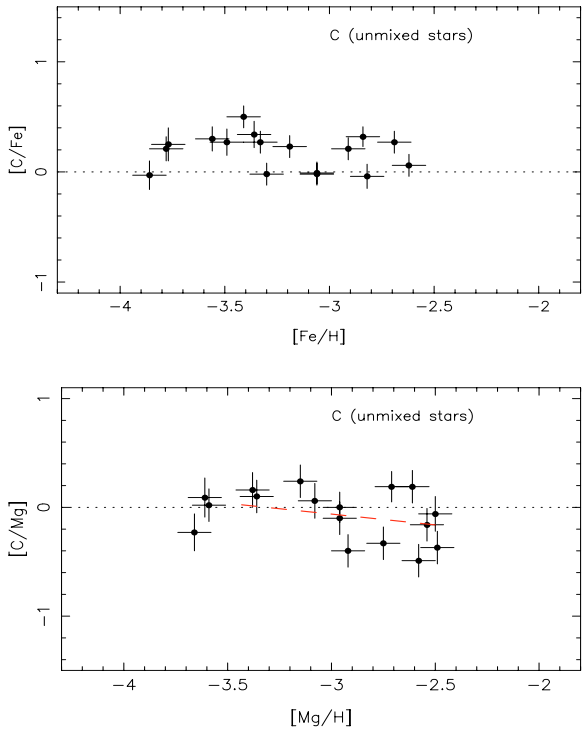

Fig. 13. [C/Fe] and [C/Mg] vs. [Fe/H] and [Mg/H] for the unmixed stars. [C/Mg] may increase slightly towards lower metallicity; for [Mg/H] < −2.9, ⟨[C/Mg]⟩ ≈ 0.0 dex.

[Fe/H] relation is remarkably flat; [C/Fe] ≈ +0.18 ± 0.16 dex over the entire range −4.0 < [Fe/H] < −2.5. The dispersion of the [C/Mg] ratios is only slightly larger than for [C/Fe]; a mild decrease of [C/Mg] with increasing metallicity is suggested.

Akerman et al. (2004) recently studied the variation of the [C/O] ratio vs. [O/H] in metal-poor halo stars. At low metallicity ([O/H] < −2.0), [C/O] is expected to decrease because O from massive supernovae increasingly dominates the enrichment process, while C is produced in stars of all masses. However, Akerman et al. (2004) found no decrease in [C/O] at low metallicity; on the contrary, [C/O] appeared to actually increase below [O/H] = −1.5, possibly to near-solar values at the lowest metallicities.

Figure 14 shows [C/O] vs. [O/H] for the combined data set; our stars extend to much lower metallicities than those of Akerman et al. Although the O and C indicators used in these two studies are completely different (high-excitation C and O lines in Akerman et al., CH and [OI] lines in our case), the results agree nicely where the samples overlap. Our XMP stars confirm that [C/O] increases to near solar values at very low metallicity.

Figure 14 also shows the predictions of different chemical evolution models, following Akerman et al. (2004):

- Their standard model using the Meynet & Maeder (2002) yields for massive stars ($8 \le M \le 80\ M_\odot$) and the Kroupa et al. (1993) IMF (dotted line).
- Their standard model with the same IMF, but C and O yields from Chieffi & Limongi (2002) for metallicities $0 \le z \le 10^{-5}$ (dashed line). Chieffi & Limongi (2002) argue that the ejecta of metal-free supernovae should be carbon rich, because the high core temperature in these stars during helium burning would favour the reaction $^4\mathrm{He}(2\alpha,\gamma)^{12}\mathrm{C}$ over $^{12}\mathrm{C}(\alpha,\gamma)^{16}\mathrm{O}$.
- The same model and Chieffi & Limongi yields, but with a top-heavy IMF ($M \ge 10\ M_\odot$; solid line).

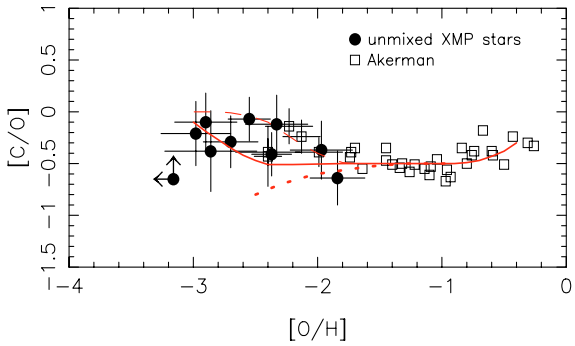

Fig. 14. [C/O] vs. [O/H] for our unmixed stars (dots) and the halo stars from Akerman et al. (2004; squares). The lines show the predictions of their standard model for C and O, using the yields of Meynet & Maeder (2002, dotted), Chieffi & Limongi (2002, dashed), and Chieffi & Limongi with a top-heavy IMF ($M > 10\ M_\odot$, solid line). The data seem to favour substantial early C production in massive zero-metal supernovae.

Our new data suggest that the best model would be somewhere between the last two of these.

5.2. Nitrogen and the [N/α] ratio

Figure 15 shows [N/Fe] and [N/Mg] vs. [Fe/H] and [Mg/H] for the subsample of unmixed stars. The trends of these ratios are not compatible with secondary N production in the early Galaxy: instead, a decrease of [N/Mg] and [N/Fe] with decreasing metallicity would be expected. The early production of N was thus primary. It may be due to massive stars where it would be induced, e.g., by mixing between the C producing regions and the H burning layer where C is transformed into N. But it could also be due to contributions by AGB stars.

- Figure 15 appears to show that the mean values of [N/Fe] and [N/Mg] decrease with increasing metallicity, perhaps reflecting a decrease in N production relative to both Fe and Mg (the [C/Mg] ratio shows a similar trend, but it is much weaker and not significant). The scatter in both relations is much larger than for both [C/Fe] and [C/Mg] (see Fig. 13). Similarly to the case of C, the scatter in [N/Mg] increases markedly with increasing [Mg/H] from about [Mg/H] = −3.
  However, were our N measurements to suffer from *metallicity-dependent* systematic errors, a spurious slope might result. 3D effects in model atmopheres (see Sect. 3.2.3) might cause such metallicity-dependent errors. However, although one cannot yet be certain, it is unlikely that differential effects in stars with [Mg/H] between −2.8 and −3.8 could vary the N abundance by the 0.5 dex needed to eliminate the observed slope (Asplund 2004). Moreover, such a systematic effect could not explain the increased dispersion of [N/Fe] and [N/Mg] towards higher metallicity.

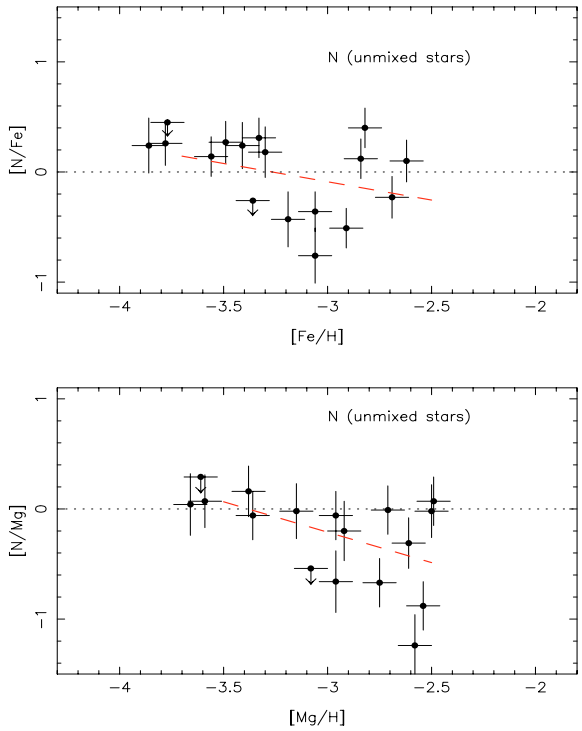

Fig. 15. [N/Fe] and [N/Mg] vs. [Fe/H] and [Mg/H] for our unmixed stars. With increasing metallicity, [N/Fe] and [N/Mg] decrease (dashed lines) and the dispersion increases, a behaviour unexpected from theoretical expectations.

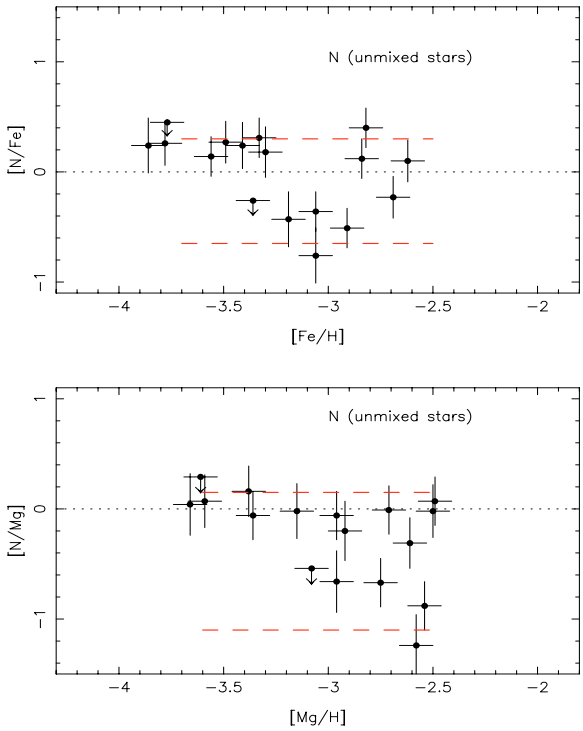

Fig. 16. The same data as in Fig. 15, but interpreted differently. We assume here that the low dispersion at low metallicity is a spurious effect due to the small size of the sample, while [N/Fe] and [N/Mg] in general shows large scatter from star to star, with $0.7 < [N/Fe] < 0.3$ and $-1.1 < [N/Mg] < 0.2$ as seen for $[Fe/H] > -3.3$.

Such a decrease of the nitrogen production with increasing metallicity is not predicted by any massive-star yields at low metallicities.

– Another interpretation is possible, however (Fig. 16): we have only five N abundance measurements (plus two upper limits) in the interval $-3.7 < [Mg/H] < -3$ where the dispersion seems to vanish, so the absence of a spread at low metallicity could be just a statistical effect. If so, the mean slope drawn in Fig. 15 would not be real, and [N/Mg] and [N/Fe] would simply vary from star to star without any mean trend (Fig. 16). Two possible explanations are:
i) the maximum [N/Mg] value (∼0.0) reflects the primary N production by normal massive supernovae, but with some stars showing much lower production. N is not easily produced in massive SNe, and the yields may depend critically on various parameters, such as rotation (Maeder & Meynet 2002), explaining the spread in the observed N abundance. The spread seems to appear at less extreme deficiencies ($[Fe/H] > -3.4$), reflecting the yields of later, i.e. lower-mass supernovae;
ii) the lowest N abundances in our stars might represent galactic gas enriched by SNe II, but before any enrichment by massive AGB stars. The majority of the N-rich stars in Fig. 16 would then be formed from matter more or less enriched by AGB winds, and the scatter in the N abundances would arise from local, inhomogeneous N enrichment of the gas from which our stars formed. In this case, metallicity would not be a good indicator of age. Moreover, we would then expect the *s*-process elements to be more abundant in N-rich than in N-poor unmixed stars. A preliminary analysis shows no clear difference in *s*-process abundances between the two sets of stars; this will be discussed in more detail in a forthcoming paper on the neutron-capture elements in our XMP stars (François et al. 2004, in prep.; Paper VII).

In both tentative explanations there remains to explain why the interstellar medium is enriched in N up to a fixed maximum ([N/Fe] ≈ 0.3 dex and [N/Mg] ≈ 0.2 dex), as clearly seen in Fig. 16.

5.3. Comparison of halo stars and DLAs

We have argued that the N abundance in our unmixed XMP stars is very close to that of the gas from which the stars were formed. The stars on the lower RGB have possibly experienced the first dredge-up (if any), but this should only affect the [N/Fe] or [N/Mg] ratios slightly (Gratton et al. 2000), even in rapidly rotating stars (Meynet & Maeder 2002).

We now compare our results to the [N/α] ratios in DLAs and extragalactic H II regions (or Blue Compact Galaxies, BCGs). E.g., both Prochaska et al. (2002) and Centurión et al. (2003) suggest the existence of a plateau at [N/α] ∼ −1.5 dex in addition to the well-known one at [N/α] = −0.8 dex, which is common to DLAs and BCGs.

Figure 17 shows [N/O] vs. [O/H] for our unmixed XMP giants, the metal-poor dwarfs studied by Israelian et al. (2004),

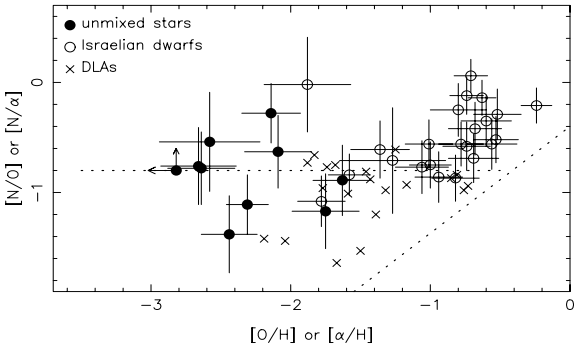

Fig. 17. Light-element abundance ratios in metal-poor dwarfs (Israelian et al. 2004, open circles), in our unmixed giants (filled circles), and in DLAs (crosses). [N/O] vs. [O/H] is shown for the stars, [N/α] vs. [α/H] for the DLAs, following Centurión et al. (2003), where α may denote O, S, or Si in different DLAs. The DLAs with [α/H] < -2 have [N/α] ≈ -1.4, while the most metal-poor stars have [N/α] ≈ -0.8; but given the scatter in both samples, this difference may not be significant. The horizontal and sloping dotted lines show the relations for primary and secondary N production, respectively. Neither sample shows any dependence of N abundance on metallicity for [O/H] or [α/H] < -1.0 dex; thus, early N production was mainly primary.

and the DLAs studied by Centurión et al. (2003) and Molaro et al. (2003). Because O abundances have been measured in very few DLAs, we plot [N/α] vs. [α/H] for the DLAs (where α is O, S, or Si, depending on the DLA), which should be equivalent to [N/O] vs., [O/H] (Molaro 2003). Error bars have been omitted for the DLAs, but the (*internal*) error of [N/α] in DLAs is claimed to be of order 0.02 dex.

In addition to the internal errors, systematic uncertainties affecting the two sets of observations include:

(i) The stellar data are subject to the neglect of 3D effects in our 1D atmospheres; using 3D models (see Sect. 3.2.2) would reduce the O abundance by typically ∼0.2 dex, but without a full 3D computation for the NH molecule the net effect on [N/O] is difficult to assess. In addition, our absolute N abundances also depend on the uncertain physical parameters for the NH band (see Sect. 3.2.3) and were corrected by −0.4 dex to force agreement with abundances from the CN band. Systematic offsets in our N/O ratios can therefore neither be excluded nor assessed quantitatively at present. New, accurate values of gf and dissociation energy for NH as well as studies of 3D model atmosphere effects on the band strength are urgently needed.

(ii) The DLA observations are affected by uncertain dust corrections. In particular, Si is easily locked onto grains, and the DLAs for which Si was used to represent O are subject to larger uncertainties.

For stars of higher metallicity ([O/H] > -1.8), the significant slope of [N/O] vs. [O/H] is indicative of secondary N production (Israelian et al. 2004). While noting the possible systematic errors, we find most of our unmixed stars to have [N/O] ∼ −0.9, similar to the metal-poor stars of Israelian et al. (2004) but extending to much lower [O/H] values. This seems to agree also with the main [N/α] plateau of the DLAs. However, while the DLA data hint at the existence of two distinct plateaus, the stars also occupy the region between them. Note also that none of our stellar [N/O] ratios is below the "lower" [N/α] plateau of the DLAs.

The similarities and differences between our stellar sample and the DLAs can be summarised as follows:

Similarities:

1. Both stars and DLAs form a well-populated plateau at [N/O] ∼ −0.9, independent of metallicity;
2. No star or DLA is found with [N/O] < -1.5.

Differences:

1. The stellar data extend to lower metallicity than DLAs, with [N/O] ∼ −0.9 at the lowest values of [O/H].
2. Even when excluding the N-rich stars (as in Fig. 17), [N/O] in stars scatters more than in DLAs.

Given the scatter of [N/O] in both stars and DLAs, these differences may not be significant, however.

Given the still-limited amount of data, it may be premature to attempt to fit all of these facts into a simple and coherent picture. We believe, however, that the lack of any significant trend of [N/O] with metallicity in both stars and DLAs requires primary N production in both. In Fig. 17 the dotted lines indicate the relations for primary and secondary N production from Centurión et al. (2003). For [O/H] < -2, the mean value of [N/O] is close to the primary production line, which suggests that massive stars have enriched the ISM in N before our very old XMP stars and DLAs were formed.

There is, however, no conclusive evidence whether the main site of this primary N production is massive Pop III stars (exploding as SNe II), AGB stars, or AGB supernovae (SN I.5). On the one hand, the positive correlation of [N/H] with [O/H] suggests an origin in massive stars, despite the large scatter in [N/O]. On the other hand, the large spread in [N/O] among Galactic stars might suggest that early AGB stars could play an important role. It may well be that N is produced in comparable amounts in *both* massive stars and AGB stars.

6. Conclusions

6.1. Internal mixing

Our careful analysis of CNO and Li abundances in extremely metal-poor giants from high-quality spectra has demonstrated that they fall cleanly in two groups:

– The first group shows clear signs of mixing of significant amounts of CN-cycle products to the surface, very similar to the extra mixing found by Gratton et al. (2000) in moderately metal-poor field giants. Evidence for this includes the non-detection of Li and low [C/N] in stars with low log g values: these stars belong to the upper RGB or the HB. No signature of ON cycle processing is detected in the mixed stars. A forthcoming paper will discuss the $^{12}C/^{13}C$ ratio to further study the extent of mixing in these stars.

– The second group shows no signature of mixing with CNO burning layers: $N_{\rm Li} > 0.14$ and [C/N] > -0.6. These stars have higher log g and lie on the lower RGB. They may still have experienced the first dredge-up, but this is expected to change their atmospheric C and N abundances very little (Gratton et al. 2000), or not at all (Denissenkov & Weiss 2004).

The mixed and unmixed stars have approximately the same value of [(C+N)/Fe] $\approx +0.25$ dex, indicating that the difference between the two groups could be entirely due to internal mixing with CN-processed material. We thus confirm the results on extra-mixing by Gratton et al. (2000) and extend them towards lower metallicity.

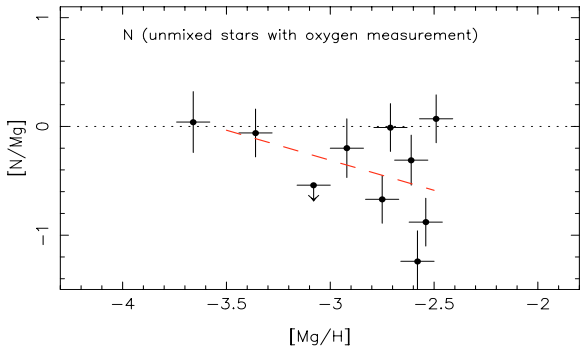

Fig. 18. Same as Fig. 15, but only for stars included in Fig. 17. The general decrease of [N/Mg] with [Mg/H] and the different behaviors of [N/Mg] and [N/O] remain visible.

6.2. The unmixed subsample

We find that the C and N abundances in the *unmixed* XMP stars should be close to those of the gas from which they were formed. These abundances thus provide useful constraints on the yields of the first stars (Pop III supernovae, early AGBs, AGB supernovae,...) and on any trends of these yields with metallicity and perhaps time.

– The [C/Fe] ratio is remarkably constant with [Fe/H] and shows only moderate scatter. [C/Mg] and [C/O] decrease slightly with metallicity from solar values at [Mg/H] ≈ -3.5 and [O/H] ≈ -3.0, respectively. We thus confirm the trends suggested by Akerman (2004) and extend them to even lower metallicity.
– The N abundances show large scatter, and the sample of unmixed stars is limited in size; the abundance trends are therefore difficult to verify and interpret. While the mean values of both [N/Fe] and [N/Mg] appear to decrease with increasing metallicity (Fig. 15), this could be just a statistical effect. In any case, the observed trends are incompatible with secondary N production in the early Galaxy.
  Our sample of unmixed XMP stars shows ranges of $-1.1 <$ [N/Mg] < -0.0 and $-0.8 <$ [N/Fe] $< +0.2$ (Fig. 16). Two tentative interpretations of this large spread are suggested:
  i) the primary N production by SNe II is close to the lower value of [N/Mg] (-1.1), and stars with higher [N/Mg] values would be formed from material enriched by the winds of massive AGB stars; or
  ii) the primary N production by SNe II is close to the higher value of [N/Mg] (0.0), explaining the [N/Mg] ratio in most of our XMP stars. However, this primary production depends critically on various parameters and could be less active in some cases, especially in less massive supernovae. Some stars would then become "nitrogen-poor".
  In order to test these different interpretations of the trends of [N/Mg] and [N/Fe] vs. metallicity, it would be important to measure the N abundances in a larger sample of XMP stars (especially for [Fe/H] < -3.4 or [Mg/H] < -3.2) to ascertain whether the small spread of [N/Fe] and [N/Mg] at very low metallicity is real or just a statistical effect.
– A diagram of [N/O] vs. [O/H] for the same stars shows no visible trend in the range $-2.8 <$ [O/H] < -1.6, but the dispersion is very large ($\sigma = 0.31$). The different behaviour of [N/Mg] and [N/O] is surprising, because both O and Mg are thought to be α elements. Because O was measurable in fewer stars than Mg, we have repeated the comparison using only stars with both Mg and O abundances (Fig. 18). As seen, the slope of [N/Mg] versus [Mg/H] remains visible. Although the sample is small, the different trends in [N/Mg] and [N/O] seem hard to explain as just a statistical effect; they are are probably real and do not favor secondary production of N.
– We have compared the [N/O] ratios in our XMP stars with [N/α] data for DLA systems. The metallicity ranges of the two samples are complementary. In spite of the large scatter, the weight of the evidence suggests that the N production was primary, especially in the first phases of Galactic evolution. It cannot yet be decided, however, whether this primary N production was due to massive Population III supernovae, AGB stars, or perhaps AGB supernovae (SN I.5); all three sources may play significant roles.

The absolute values of the measured abundances are susceptible to various uncertainties, from inaccuracy of the molecular parameters to the effects of simplified models (LTE and 1D approximations). However, these systematic effects should be similar from star to star and the derived trends remain robust. It is important, however, to verify the effects of 3D NLTE model effects and improved molecular data on the derived abundances as soon as possible.

As another item for the future, we have found that the abundance anomalies observed in the "mixed" stars are due to mixing between their surfaces and CNO-processing layers, similar to the scenario (extra mixing) inferred by Gratton et al. (2000) and theoretically explained by, e.g. Charbonnel (1995) and Denissenkov & VandenBerg (2003 and references therein). However, we cannot completely rule out the possibility that the observed anomalies could result from pollution by AGB binary companions. It would thus be interesting to search for any companions of the mixed stars (radial velocities, astrometric orbits, or interferometry) in order to check this alternative.

Acknowledgements. We thank the ESO staff for assistance during all the runs of our Large Programme. T.C.B. acknowledges partial funding for this work from grants AST 00-98508 and AST 00-98549, as well as from grant PHY 02-16783: Physics Frontiers Center/Joint Institute for Nuclear Astrophysics (JINA), awarded by the US National Science Foundation. B.N. and J.A. thank the Carlsberg Foundation and the Swedish and Danish Natural Science Research Councils for partial financial support of this work.

References

Akerman, C. J., Carigi, L., Nissen, P. E., Pettini, M., & Asplund, M. 2004, A&A, 414, 931
Alonso, A., Arribas, S., & Martínez-Roger, C. 1998, A&AS, 131, 209
Alonso, A., Arribas, S., & Martínez-Roger, C. 1999, A&AS, 140, 261
Alvarez, R., & Plez, B. 1998, A&A, 330, 1109
Asplund, M. 2004, Mem SAI, 75, 300
Asplund, M., & García Pérez, A. E. 2001, A&A, 372, 601
Barbuy, B., Meléndez, J., Spite, M., et al. 2003, ApJ, 588, 1072
Asplund, M., Gustafsson, B., Kiselman, D., & Eriksson, K. 1997, A&A, 318, 521
Ballester, P., Modigliani, A., Boitiquin, O., et al. 2000, ESO Messenger, 101, 31
Beers, T. C. 1999, in Third Stromlo Symposium: The Galactic Halo, ed. B. Gilson, T. Axelrod, & M. Putman, ASP Conf. Ser., 165, 206
Beers, T. C., Preston, G. W., & Shectman, S. A. 1992, AJ, 103, 1987
Bond, H. E. 1980, ApJS, 44, 517
Carbon, D., Barbuy, B., Kraft, R. P., Friel, E., & Suntzeff, N. B. 1987, PASP, 99, 335
Cayrel, R., Depagne, E., Spite, M., et al. 2004, A&A, 416, 1117 (Paper V)
Centurión, M., Molaro, P., Vladilo, G., et al. 2003, A&A, 403, 55
Charbonnel, C. 1995, ApJ, 453, L41
Chiappini, C., Matteucci, F., & Meynet, G. 2003, A&A, 410, 257
Chiappini, C., Romano, D., & Matteucci, F. 2003, MNRAS, 339, 63
Chieffi, A., & Limongi, M. 2002, ApJ, 577, 281
Cowan, J. J., Sneden, C., Burles, S., et al. 2002, ApJ, 572, 861
Dekker, H., D'Odorico, S., Kaufer, A., et al. 2000, in Optical and IR Telescopes, Instrumentation and Detectors, ed. I. Masanori, & F. A. Morwood, Proc. SPIE, 4008, 534
Denissenkov, P. A., & VandenBerg, D. A. 2003, ApJ, 593, 509
Denissenkov, P. A., & Weiss, A. 2004, ApJ, 603, 119
Depagne, E., Hill, V., Spite, M., et al. 2002, A&A, 390, 187
Edvardsson, B., Andersen, J., Gustafsson, B., et al. 1993, A&A, 275, 101
Gratton, R., Sneden, C., Carretta, E., & Bragaglia, A. 2000, A&A, 354, 169
Grevesse, N., & Sauval, A. J. 1998, Space Sci. Rev., 85, 161
Gustafsson, B., Bell, R. A., Eriksson, K., & Nordlund, Å. 1975, A&A, 42, 407
Gustafsson, B., Edvardsson, B., Eriksson, K., et al. 2003, in Stellar Atmosphere Modeling, ed. I. Hubeny, D. Mihalas, & K. Werner, ASP Conf. Ser., 288, 331
Henry, R. B. C., Edmunds, M. G., & Köppen, J. 2000, ApJ, 541, 660
Huang, Y., Barts, S. A., & Halpern, J. B. 1992, J. Phys. Chem., 96, 425
Huber, K. P., & Herzberg, G. 1979, Constants of Diatomic Molecules (New York: van Nostrand Reinhold)
Israelian, G., Ecuvillon, A., Rebolo, R., et al. 2004 [arXiv:astro-ph/0405049]
Izotov, Y. I., & Thuan, T. X. 1999, ApJ, 511, 639
Kobulnicky, H. A., & Skillman, E. D. 1996, ApJ, 471, 211
Korn, A. J., Shi, J., & Gehren, T. 2003, ApJ, 407, 691
Kraft, R. P. 1994, ApJS, 106, 553
Kroupa, P., Tout, C. A., & Gilmore, G. 1993, MNRAS, 262, 545
Kurucz, R. L. 2001, in http://cfaku5.harvard.edu/programs/atlas9/molec.dat
Laird, J. B. 1985, ApJ, 289, 556
McWilliam, A., Preston, G. W., Sneden, C., & Searle, L. 1995, AJ, 109, 2757
Meynet, G., & Maeder, A. 2002, A&A, 381, L25
Molaro, P. 2003, in CNO in the Universe, ed. C. Charbonnel, D. Schaerer, & G. Meynet, ASP Conf. Ser., in press [arXiv:astro-ph/0301407]
Molaro, P., Centurión, M., D'Odorico, V., & Péroux, C. 2003, in Origin and Evolution of the Elements, Carnegie Observatories, Pasadena, ed. A. McWilliam [arXiv:astro-ph/0307173]
Nissen, P. E., Primas, F., Asplund, M., & Lambert, D. 2002, A&A, 390, 235
Norris, J. E., Ryan, S. G., & Beers, T. C. 2001, ApJ, 561, 1034
Norris, J. E., Ryan, S. G., Beers, T. C., Aoki, W., & Ando, H. 2002, ApJ, 569, 107
Pilachowski, C. A., Sneden, C., & Booth, J. 1993, ApJ, 407, 699
Pilachowski, C. A., Sneden, C., & Kraft, R. P. 1996, AJ, 111, 1689
Pilyugin, L. S., Thuan, T. X., & Vílchez, J. M. 2003, A&A, 397, 487
Plez, B. Brett, J. M., & Nordlund, Å. 1992, A&A, 256, 551
Pradhan, A. D., Partridge, H., & Bauschlicher, C. W., Jr. 1994, J. Chem. Phys., 101, 3857
Prochaska, J. X., Henry, R. B., O'Meara, J. M., et al. 2002, PASP, 114, 933
Sneden, C. 1973, ApJ, 184, 839
Sneden, C., McWilliam, A., Preston, G. W., et al. 1996, ApJ, 467, 819
Sneden, C., Cowan, J. J., Ivans, I. I., et al. 2000, ApJ, 533, L139
Sneden, C., Cowan, J. J., Lawler, J. E., et al. 2003, ApJ, 591, 936
Tomkin, J., & Lambert, D. L. 1984, ApJ, 279, 220